Sintering of 3 mol % Y_2O_3–TZP and its fracture after ageing treatment

SAN-YUAN CHEN, HONG-YANG LU
Materials Research Laboratories, Industrial Technology Research Institute, Chutung 31015, Taiwan, R.O.C.

TZP ceramic of 99.7% theoretical relative final density was obtained by pressureless sintering a commercial co-precipitated 3 mol % Y_2O_3–ZrO_2 powder at 1400° C for 10 h. Fracture surfaces of the aged material revealed that the fracture of TZP ceramic was typified by an intergranular mode in areas where the phase was mainly tetragonal, whereas the transgranular mode was found predominantly in the area containing more monoclinic phase. Microcracks induced by the (t) → (m) transformation provided short paths for water to accelerate the property degradation of TZP upon low-temperature ageing in a humid atmosphere.

1. Introduction

Y_2O_3–tetragonal zirconia polycrystal (Y–TZP) is a potential contender for structural applications. 3 mol % Y_2O_3–TZP has particularly been widely studied due to its extremely high strength (~ 1500 MPa) [1] and high fracture toughness (~ 22 MPa $m^{1/2}$) [2]. However, the (t) → (m) transformation induced on ageing at 200 to 300° C resulted in a detrimental strength degradation [3–8] The mechanical strength deterioration was further accelerated when Y–TZP was exposed to a humid atmosphere [9–15]. The (t) → (m) transformation is known [4, 12, 16] to be strongly dependent upon its Y_2O_3 content and grain size. For 3 mol % Y_2O_3 addition, the strength degradation was inhibited when the grain size of TZP was reduced to < 0.5 μm [7] by sintering at 1500° C for 2 h [17].

The ageing behaviour of Y–TZP [16, 18], suggested that the (t) → (m) transformation occurred from the sample surface inwards to the interior. Also, microcracks [7] and macrocracks [5] were generated from the (t) → (m) transformation in the aged samples. Sato *et al.* [13, 19] pointed out that for 2 mol % Y_2O_3, flexural strength decreased appreciably only when the transformed (m)-ZrO_2 thickness exceeded ~ 50 μm.

Microstructure studies have concentrated on the (t) → (m) transformation analysis using TEM [1, 14, 20, 21]. Attention was paid in this study to the fracture mode in the light of understanding the low-temperature strength degradation of Y–TZP. We report the sintering of 3 mol % Y_2O_3–TZP and its fracture surface morphology when aged samples were subjected to the three-point bending test.

2. Experimental procedure

TZ3Y ZrO_2 powder (Toyo Soda Co. Ltd, Tokyo) containing trace impurities of SiO_2 (100 p.p.m.), Fe_2O_3 (20 p.p.m.) and Na_2O (70 p.p.m.) was used in this study. Discs were dry-pressed at pressures of 100 MPa to 15 mm diameter and sintered at 1400, 1500 and 1600° C for a period of 0.5 to 20 h. Samples were furnace-cooled to room temperature. Sintered samples were subsequently aged at 100 to 500° C for several minutes to 500 h in air of a relative humidity of ~ 80%. These samples were then analysed by X-ray diffraction (XRD) using Cu$K\alpha$ radiation at 40 kV and 20 mA. The estimation of phase content ratio, i.e. the ratio of (monclinic)/(monoclinic + tetragonal), following Garvie and Nicholson [22], was based on measuring the peak heights of tetragonal (1 1 1), monoclinic (1 1 $\bar{1}$) and (1 1 1) by scanning through 2θ angles of 26 to 33°. The variation of (m)-ZrO_2 content with sample thickness was determined by the XRD method [22] on aged TZP samples when the surface was removed successively by using ~ 10 μm SiC slurry.

The final density ϱ_f of the sintered body was determined by Archimedes method; water was used as the immersion medium. Samples for SEM observation were prepared by lapping with diamond paste successively from 15 to 1 μm after grinding, followed by thermal etching at 1400° C for 1 h to delineate grain boundaries. The average grain size of the sintered body was estimated by measuring lineal intercepts on SEM micrographs according to the technique developed by Mendelson [23]. A notch was cut by a 100 μm thick diamond saw before samples were fractured by three-point bending. Fracture surfaces coated with a thin Au–Pd layer were then observed by SEM. Bend bars of 3 mm × 4 mm × 40 mm were prepared according to the Japanese Standard JIS R1601 (1981). Their surface was ground down to 250 μm finish by diamond wheels. Flexural strength was measured by the four-point bending test with a 30 mm outer span and a 10 mm inner span, where the crosshead speed was fixed at 0.5 mm min^{-1}. Fracture toughness was determined by the Vickers microindentation technique by using a 490 N load, and its value calculated by the equation of Niihara *et al.* [24].

3. Results

3.1. Sintering

Final densities of > 99.0% theoretical were obtained

0022–2461/88 $03.00 + .12

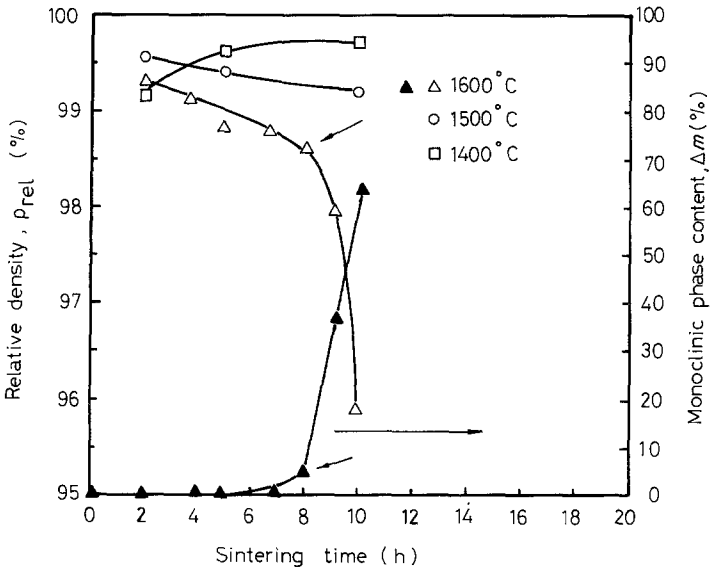

Figure 1 (m)-ZrO_2 content, increasing abruptly as the relative final density decreased. (▲, △) 1600° C; (○) 1500° C; (□) 1400° C.

for samples sintered at 1400 and 1500° C for up to 10 h. However, the final density was found to decrease with longer dwelling time for sintering at 1500 and 1600° C. Only those sintered at the lower temperature of 1400° C experienced a gradual increase of the final density with sintering time to ϱ_{rel} = 99.7% for 10 h sintering. As shown arrowed in Fig. 1, the densities of samples sintered at 1600° C manifested a sharp drop from 99.4 to 95.8% when the dwelling time was extended from 8 h to 10 h. Sintered samples contained ~ 100% tetragonal phase except those sintered at 1600° C for longer than 8 h (Fig. 1). The (m)-ZrO_2 content also appeared to increase abruptly at the point where the decrease of the final sintered density was appreciable (arrowed in Fig. 1).

The average grain size of the sintered samples increased progressively as the sintering proceeded (Fig. 2). Grain growth became more appreciable when samples were sintered at 1600° C. The average grain size was doubled when the sintering time increased from 2 h to 10 h. The point where the (t)-ZrO_2 content decreased sharply appeared at ~ 8 h sintering and the average grain size was ~ 1.35 μm (arrowed in Fig. 2). The (m)-ZrO_2 content was ~ 70% for samples sintered for 10 h. However, those sintered at 1400 and 1500° C still contained ~ 100% tetragonal even after 20 h sintering.

Apart from those sintered at 1600° C, the as-sintered TZP featured a rather uniform microstructure (Fig. 3). Occasionally large (c)-grains were observed (arrowed) which appeared to have grown by a coalescence mechanism.

3.2. Ageing and mechanical properties

The ageing kinetics of 3 mol % Y_2O_3–TZP had a sigmoidal shape as previously reported [17]. The accelerating effect of water on the ageing of TZP appeared to be pronounced as previously reported [9–13]; detailed studies of the kinetics will be reported elsewhere [14]. Table I illustrates the amount of (m)-ZrO_2 when samples were aged in different atmospheres. For samples with a G_{av} = 0.52 μm, ageing in a water atmosphere resulted in 25% (m)-ZrO_2, whereas no detectable (m)-ZrO_2 was found when ageing was in air or in a vacuum of 13.1 nPa (10^{-5} torr).

The fracture toughness (K_{Ic}) of as-sintered TZP was

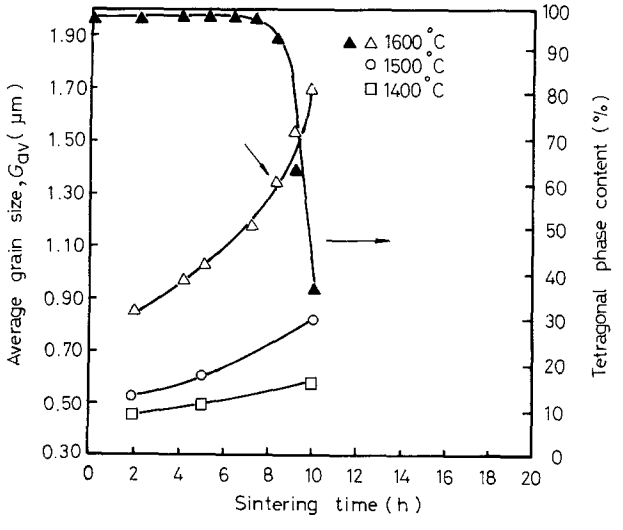

Figure 2 (t)-ZrO_2 content, decreasing sharply when sintered at 1600° C for 8 h. (▲, △) 1600° C; (○) 1500° C; (□) 1400° C.

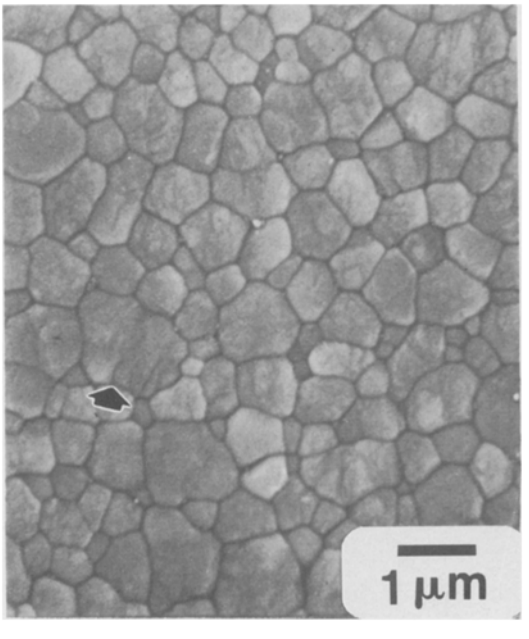

Figure 3 Microcrack-free 3 mol % Y_2O_3–TZP, with large (c)-grains appearing to have grown by a coalescence mechanism.

TABLE I Atmospheric effect on ageing of 3 mol % Y_2O_3–TZP*

Ageing atmosphere	Δm-ZrO_2 (%)					
	Grain size 0.52 μm		Grain size 0.58 μm		Grain size 1.15 μm	
	Aged 5 h	Aged 20 h	Aged 5 h	Aged 20 h	Aged 5 h	Aged 20 h
Vacuum	0	0	0	3	29	58
Air	0	0	0	15	54	68
Water	25	–	44	–	71	–

*1500° C sintered and 250° C aged.

typically in the range of 6.5 to 7.0 MPa $m^{1/2}$. When samples were subjected to ageing treatment for 168 h, the occurrence of property degradation manifested a minimum K_{Ic} of 5.0 MPa $m^{1/2}$ at 250° C. Fig. 4 reveals that this minimum K_{Ic} (arrowed) also coincided with the maximum (m)-ZrO_2 transformed. The bending strength of as-sintered TZP amounts to ~ 600 MPa; these samples have an average grain size G_{av} = 0.58 μm after sintering at 1500° C for 5 h. Fig. 5 shows that the minimum of bending strength again appeared at the maximum (m)-ZrO_2 transformed on ageing at 250° C. For the sample of minimum σ_f (340 MPa), the corresponding (m)-ZrO_2 content on the sample surface was ~ 70%. The (m)-ZrO_2 content decreased from the surface inwards to the sample interior. The concentration profile of (m)-ZrO_2 transformed (Δm) for samples sintered at 1600° C for 2 h and subsequently aged at 250° C for various times is presented in Fig. 6. The (t) → (m) transformation was confined to a thickness of < 10 μm from the sample surface for < 5 h ageing. On the other hand, for samples aged for 500 h the transformation zone thickness extended much further inwards to ~ 80 μm.

3.3. Microstructure and fracture mode

Extensive microcracks (Fig. 7) were observed on the surface of the aged samples. This appeared conspicuous as long as the aged samples exhibited appreciable (t) → (m) transformation. Figs 8b to e present the fracture surface on the compressive stress side of a three-point bending specimen (Fig. 8a), for a TZP ceramic aged at 250° C for 168 h. The microstructure (Fig. 8b) is characterized by a transition of the fracture mode across the sample thickness. Fig. 8b can be divided into two areas of distinguishable fracture mode by a boundary BB′. The boundary BB′ was located at ~ 40 μm from the sample surface inwards where the (m)-ZrO_2 content was ~ 12%. Transgranularly fractured large grains (indicated by X), were seen on this surface. A transitional range where fracture occurred through a mixture of the transgranular and the intergranular modes is also shown in Fig. 8c. To the left of the boundary BB′ an intergranular fracture mode is seen to be predominant. Angular-shaped grains of the (t)-symmetry were observed, which was similar to the as-sintered samples. Scattered (m)-ZrO_2 micrograins were also seen, as indicated in Fig. 8d. To the right of the boundary BB′, closer to the sample surface, the fracture mode was preponderantly transgranular. Fig. 8e presents a transgranular fracture sample with an extensive number of (m)-ZrO_2 micrograins (m).

4. Discussion

4.1. Effect of sintering on the phase content

The abrupt reduction of the final sintered density appeared coincidently with the falling of the (t)-ZrO_2 content for samples sintered for 8 h at 1600° C. An explanation is that the sintering schedule resulted in samples of average grain size G_{av} > 1.35 μm, which exceeded the critical grain size of 1 μm [25] for the (t) → (m) transformation under such a matrix constraint. The discrepancy of the theoretical densities for (m)- and (t)-ZrO_2, ϱ_m = 5560 kg m^{-3} [26] and ϱ_t = 6100 kg m^{-3} [26], can account for the decrease of the final sintered density. Average grain sizes for samples

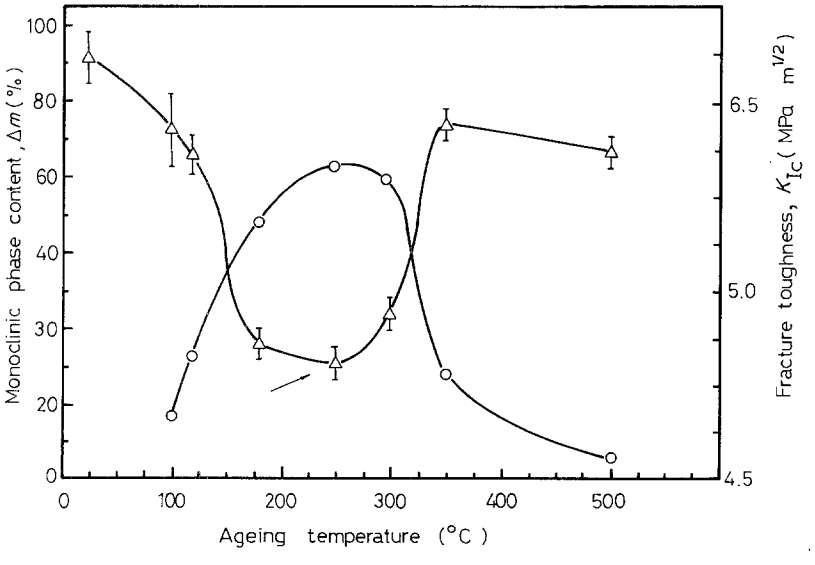

Figure 4 The coincidence of the maximum (○) (m)-ZrO_2 content and the minimum of (△) K_{Ic} occurring at 250° C ageing.

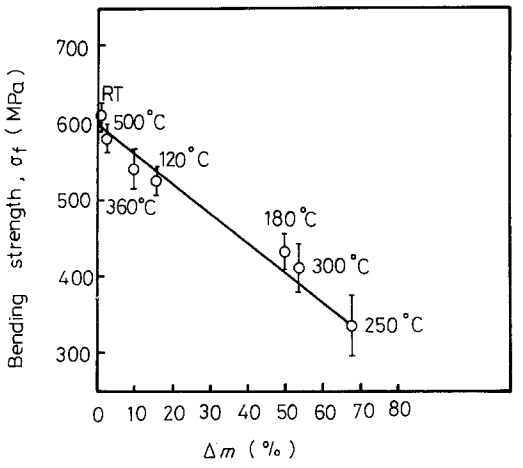

Figure 5 The minimum bending strength appearing at the maximum (m)-ZrO_2 content when aged at 250° C for 168 h. Sintered at 1500° C for 5 h; $G_{av} \approx 0.58\,\mu m$.

sintered at 1400 and 1500° C were < 0.60 and $< 0.90\,\mu m$, respectively, being below the critical value which made possible the retention of (t)-ZrO_2 (Fig. 2).

4.2. Strength degradation and fracture mode

The coincidence of the maximum transformed monoclinic phase content with both the minimum fracture toughness (K_{Ic}) and flexural strength (σ_f) suggests that the degradation of mechanical properties occurring in the aged 3 mol % Y–TZP was directly due to the (t) → (m) transformation thus induced. A mirror-image relationship can be approximated between the fracture toughness degradation and the (m)-ZrO_2 content curve with respect to the ageing temperature (Fig. 4). This gave further support to the preceding argument that the increase of (m)-ZrO_2 content resulted consequently in property degradation. In fact, Matsui *et al.* [5] and Watanabe *et al.* [4] reported similar results by ageing TZP of different solute (Y^{3+}) contents: 4.5 mol % for the former and 4 mol % for the latter. Although from this study the ageing temperature (250° C) at which the minimum σ_f occurred was different from 200 to 300° C [4, 5, 8], the strength degradation due mainly to the (t) → (m) transformation induced upon ageing is consistent and clear.

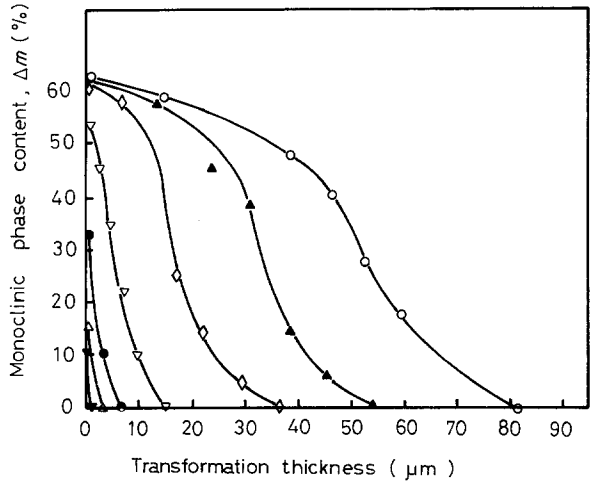

Figure 6 The concentration profile of transformed (m)-ZrO_2 content for 3 mol % Y_2O_3–TZP aged at 250° C. (▼) 40 min, (△) 2 h, (●) 5 h, (▽) 20 h, (◇) 50 h, (▲) 150 h, (○) 500 h.

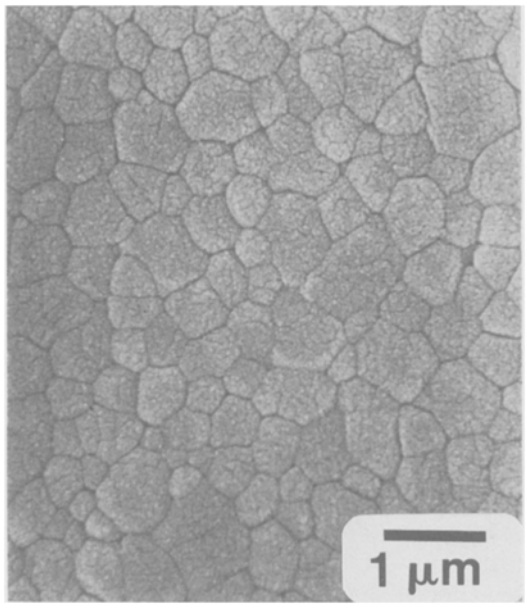

Figure 7 Extensive microcracks observed in aged 3 mol % Y–TZP.

A transgranular fracture mode was predominant in the area of high (m)-ZrO_2 content, as indicated by Fig. 8e. However, in the sample interior ($\sim 55\,\mu m$) where (t)-ZrO_2 was retained, the intergranular fracture mode prevailed. It can be concluded that the (t)-ZrO_2 grain fractured intergranularly whereas a transgranular mode was the typical fracture mode of microcracked (m)-ZrO_2 grains. Surface microcracks (Fig. 7) observed on the aged samples indicated that these microcracks existed prior to the three-point bending. Microcracking was induced on the (t) → (m) transformation apparently due to the accompanied volume expansion. When fracture occurred, the propagation of a critical crack did not appear to induce further (t) → (m) transformation, as is observed in Mg-PSZ [27], but shattered the already microcracked (m)-ZrO_2 grains. The transformation-induced microcracks [28] were involved in affecting the fracture behaviour, but their contribution was not "enhancement"; and rather to the contrary, resulted in the property degradation.

Strength degradation became appreciable only when the transformation zone exceeded $\sim 50\,\mu m$ as concluded by Matsui *et al.* [13, 19]. However, a decrease of σ_f by $\sim 10\%$ was obtained when the transformed monoclinic content reached $\sim 10\%$ for ageing at 360° C, as indicated in Fig. 5. Referring to Fig. 6, $\sim 10\%$ of monoclinic content was equivalent to a transformed thickness of only $\sim 10\,\mu m$ for ageing at 250° C. The conclusion drawn by Matsui *et al.* [13, 19] cannot be confirmed in the present investigation of 3 mol % Y_2O_3-TZP.

4.3. Atmospheric effects on ageing

The profile of the (m)-ZrO_2 content (Fig. 6) was inconsistent with that reported by Sato *et al.* [13], Iio *et al.* [18] and Miyazawa *et al.* [29]. It is clear that ageing-induced (t) → (m) transformation started from the sample surface inwards. A further implication is that the (t)-ZrO_2 particles on the surface were more unstable and susceptible to the (t) → (m) transformation than

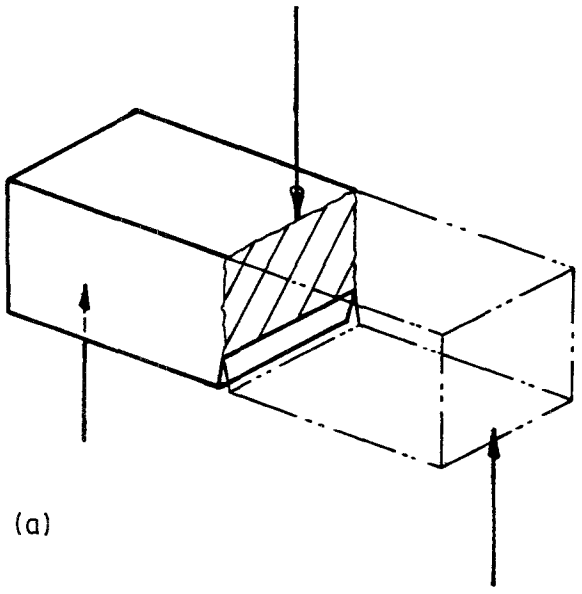

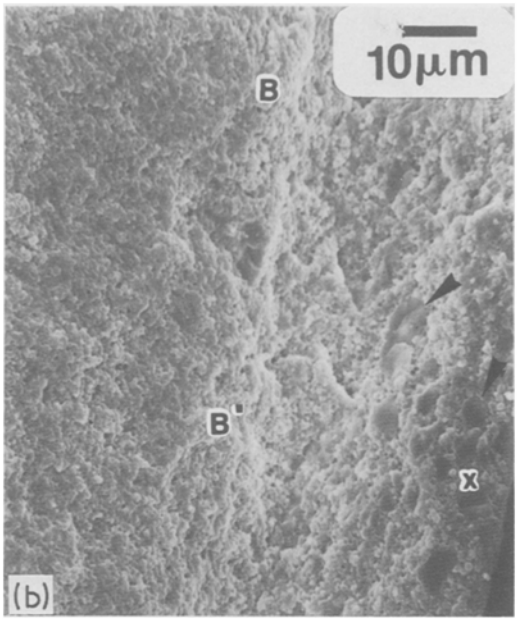

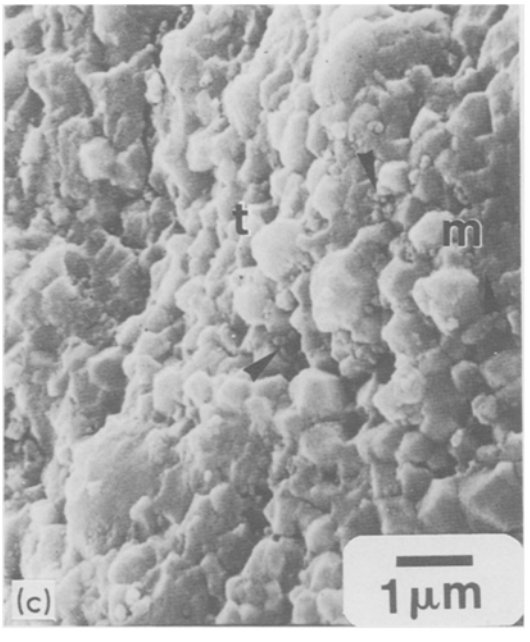

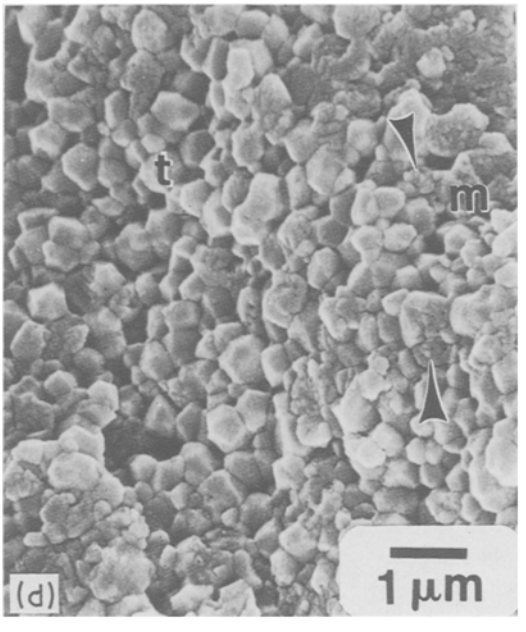

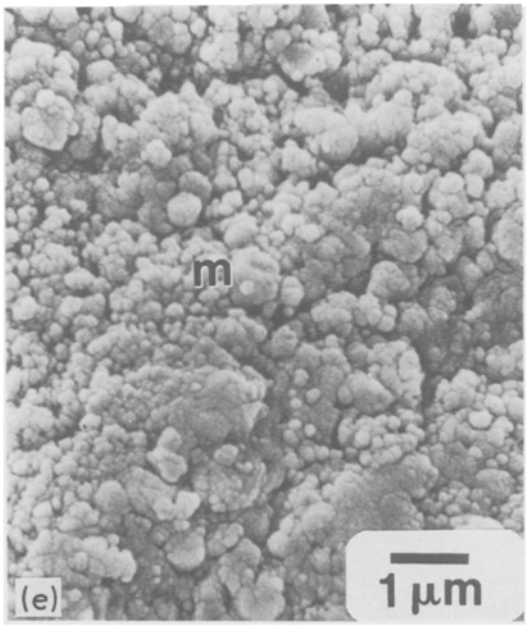

Figure 8 (a) Fracture in three-point bending. (b) Boundary BB′ of two distinguishable fracture modes in aged 3 mol % Y_2O_3–TZP. (c) A transitional range of mixed-mode fracture where (t)-ZrO_2 fractured intergranularly and (m)-ZrO_2 transgranularly. (d) Scattered (m)-ZrO_2 micrograins after fracture, appearing in the transitional range. (e) Transgranular fracture, resulting in an extensive number of (m)-ZrO_2 micrograins.

those in the bulk when they were subjected to a low-temperature ageing. The (t) → (m) transformation induced on ageing was accelerated by the water vapour present in the ageing atmosphere as previously suggested [9–13]. Our results (Table I) lend further support to this viewpoint. Microcracks provided short paths for water to accelerate the (t) → (m) transformation. The autocatalytic effect [2, 5, 21] augmented by the water acceleration would have promoted a faster kinetics of the (t) → (m) transformation; therefore ageing in a water atmosphere resulted in a higher (m)-ZrO_2 content. The evidence of microcracks (Fig. 7) induced on ageing was indeed unambiguous.

The actual accelerating mechanism of water involved, however, still remains a subject of interest [9–15].

5. Conclusions

To summarize, the following conclusions are drawn:

1. High-density 3 mol % Y_2O_3–TZP (ϱ_{rel} = 99.7%) was obtained by pressureless sintering at 1400° C for 10 h.

2. Aged 3 mol % Y_2O_3–TZP samples exhibited the fracture behaviour of two distinguishable modes from the sample surface to the interior. An intergranular mode was found predominantly in areas of high (t)-ZrO_2 content; those areas rich in (m)-ZrO_2 fractured transgranularly.

3. (m)-ZrO_2 micrograins were observed after the transgranular fracture.

4. Microcracking induced on ageing provided short paths for water to accelerate the low-temperature property degradation of 3 mol % Y_2O_3–TZP.

5. The (t) → (m) transformation, and microcracks thus induced on ageing, led to a mechanical property degradation.

Acknowledgements

Funding support by the Ministry of Economic Affairs of R.O.C. is gratefully acknowledged. Thanks are also due to Mr Liang-Ying Huang for technical assistance.

References

1. M. RUHLE, N. CLAUSSEN and A. H. HEUER, *Adv. Ceram.* **12** (1984) 352.
2. Toyo Soda Ceramics Technical Bulletin No. Z-010 (Toyo Soda Co., Tokyo, 1985).
3. K. KOBAYASHI, H. KUWAJIMA and T. MASAKI, *Solid State Ionics* **3/4** (1981) 489.
4. M. WATANABE, S. IIO and I. FUKUURA, *Adv. Ceram.* **12** (1984) 391.
5. M. MATSUI, T. SOMA and I. ODA, *ibid.* **12** (1984) 371.
6. T. SATO and M. SHIMADA, *J. Amer. Ceram. Soc.* **67** (10) (1984) C212.
7. *Idem, J. Mater. Sci.* **20** (1985) 1466.
8. T. MASAKI, *Int. J. High Tech. Ceram.* **1** (1986) 85.
9. T. SATO and M. SHIMADA, *J. Amer. Ceram. Soc.* **68** (6) (1985) 356.
10. *Idem., J. Mater. Sci.*, **20** (1985) 3988.
11. K. NAKAJIMA, K. KOBAYASHI and Y. MURATA, *Adv. Ceram.* **12** (1984) 399.
12. A. J. A. WINNBUST and A. J. BURGGRAAF, Paper 1A4, Extended Abstracts of Zirconia 86 Conference, Tokyo, Japan (1986).
13. T. SATO, S. OHTAKI, T. ENDO and M. SHIMADA, paper 3P1 as in ref. 12.
14. H. Y. LU and S. Y. CHEN, unpublished results (1986).
15. F. F. LANGE, G. L. DUNLOP and B. I. DAVIES, *J. Amer. Ceram. Soc.* **69**(3) (1986) 237.
16. K. TSUKUMA, Y. KUBOTA and T. TSUKIDATE, *Adv. Ceram.* **12** (1984) 382. (Edited by M. Ruhle, N. Claussen and A. H. Heuer, Amer. Ceram. Soc., Columbus, Ohio, USA.)
17. H. Y. LU and S. Y. CHEN, *J. Amer. Ceram. Soc.* **70**(8) (1987) 537.
18. S. IIO and M. WATANABE, paper 1A5, as in ref. 12.
19. T. SATO, S. OHTAKI, T. ENDO and M. SHIMADA, paper 1A3, as in ref. 12.
20. H. SCHUBERT and G. PETZOW, paper 1A2, as in ref. 12.
21. H. Y. LU, H. Y. LIN and S. Y. CHEN, *Ceram. Int.* in press.
22. R. C. GARVIE and P. S. NICHOLSON, *J. Amer. Ceram. Soc.* **55**(6) (1972) 303.
23. M. I. MENDELSON, *ibid.* **52**(8) (1969) 443.
24. K. NIIHARA, R. MORENA and D. P. H. HASSELMAN, *J. Mater. Sci. Lett.* **1** (1982) 13.
25. F. F. LANGE and D. J. GREEN, *Adv. Ceram.* **3** (1984) 217.
26. R. STEVENS, "An Introduction to ZrO_2", Magnesium Elektron Publication No. 113, Twickenham, England (1983).
27. D. L. PORTER and A. H. HEUER, *J. Amer. Ceram. Soc.* **60**(3/4) (1977) 183.
28. N. CLAUSSEN, J. STEEBS and R. F. PABST, *Amer. Ceram. Soc. Bull.* **56**(6) (1977) 559.
29. T. MIYAZAWA, H. MITSUTA, H. HIROI and H. OKINAKA, *Degradation and partially stabilized Zirconia,* Annual Meeting of the Japanese Society of Powder Metallurgy, Tokyo, 1983, pp. 161–2.

Received 5 January
and accepted 15 May 1987